



ELSEVIER

Journal of Photochemistry and Photobiology A: Chemistry 120 (1999) 135–140

Journal of
Photochemistry
and
Photobiology
A: Chemistry

Excitation energy transfer between dye molecules in lasing microparticles

T. Takahashi, K. Fujiwara, S. Matsuo, H. Misawa*

Graduate School of Engineering, University of Tokushima, Tokushima 770-8506, Japan

Received 15 August 1998; received in revised form 21 September 1998; accepted 22 September 1998

Abstract

Energy transfer from excited state donor to ground state acceptor dyes in polymer microparticles with a diameter of 30–60 μm was observed under lasing condition. The energy transfer efficiency was found to be higher with the increasing size of the particle. This result indicates that the excitation energy transfer efficiency can be controlled by the particle size without varying temperature and dye concentration. The dynamics of energy transfer was observed through picosecond time-resolved emission spectral measurements. © 1999 Elsevier Science S.A. All rights reserved.

Keywords: Energy transfer; Lasing microparticle; Microparticle cavity; Picosecond time-resolved spectrum; Morphology dependent resonance

1. Introduction

Excitation energy transfer from an excited state donor dye to a ground state acceptor dye plays an important role in the initial process of various photochemical reactions such as photosynthesis of green plants. The photosynthetic light-harvesting antenna in plant can absorb light and transport excitation energy through a stack of several kinds of chromoproteins to the reaction center. Langmuir–Blogett (LB) multilayer films in artificial photosynthetic molecular systems and/or molecular devices have been studied in order to control and enhance excitation energy transfer efficiency [1]. On the other hand, such an enhancement of energy transfer efficiency was observed in microparticle cavity [2–5].

It has been reported that spherical microparticles such as liquid droplets and polymer particles act as high-Q optical cavities [6–11]. In the particle cavities, light repeats an almost total internal reflection (TIR) at the boundary surface of the particle [11]. When the wavelength is of an adequate value, the light repeats TIR and returns to the starting point with the same phase, then an optical resonance occurs. Such resonances are called Morphology Dependent Resonance's (MDR's) or Whispering Gallery Mode's (WGM's). Therefore, compared with the case of the bulk materials, an interaction between matter and light inside the particle is

extremely enhanced by MDR's [12–15]. Thus, the efficiency of the energy transfer is expected to increase inside the particle cavity.

Indeed, using such features of microparticle cavities, an enhancement of the energy transfer efficiency has been reported in dye-doped microdroplet. Arnold et al. have investigated an energy transfer from Coumarin 1, which acts as a donor, to Rhodamine 6G (acceptor) [2]. Such energy transfer occurs during spontaneous emission of donor dye in the dye-doped glycerol microdroplets. They have shown that the efficiency of energy transfer inside the particle was enhanced by more than 100 times as compared with bulk solutions due to MDR. Furthermore, they have calculated the photon lifetime from the energy transfer rate dependence on acceptor concentration, and estimated Q -value [15]. Armstrong also has reported fluorescence spectral measurement data on the donor (Fluorescein 548)-doped ethanol droplets in which acceptor (Rhodamine B)-doped submicrometer particles of polystyrene were dispersed [3]. When the size of the polystyrene particles was large, the lasing light of both acceptor and donor dyes were observed, and the reabsorption mechanism was dominant for the energy transfer. However, they found that Förster energy transfer was a prominent mechanism when the size of the polystyrene particles became small. On the other hand, Leung et al. have theoretically examined the enhanced energy transfer in the particle by assuming the reabsorption mechanism, and reported that efficiency of energy transfer strongly depended on its Q -value [4].

*Corresponding author. Tel.: +81-886567389; fax: +81-886567598; e-mail: misawa@eco.tokushima-u.ac.jp

Such enhanced energy transfer in individual microparticles is very important in sensitized photochemistry and in energy transfer near the surface of biological membranes. If we could control this energy transfer efficiency arbitrarily, construction of efficient micro-photochemical reactors, tunable micro-laser light source, and so on would be possible. In this article, we report energy transfer efficiency dependence on particle size by measuring emission spectra under lasing condition in both donor and acceptor dyes-doped poly(methylmethacrylate) (PMMA) particles, which have stable morphology and high optical quality. Also, time-resolved fluorescence spectra were measured.

2. Experiment

2.1. Sample preparation

The crosslinked PMMA (Soken Kagaku, MR-60G, 30–60 μm diameters) particles were used in the present study. Rhodamine 6G (Rh6G; Exciton) and 3,3'-diethyloxadicyanobenzene iodide (DODCI; Exciton) dyes were doped into the particles as the donor and acceptor, respectively. The PMMA particles (50 mg) were dispersed for 48 h in the acetone–methanol solution (50/50 v/v, 5 ml) of Rh6G (1.0×10^{-2} M) and DODCI (1.0×10^{-3} M) to make the donor–acceptor doped polymer particles. Then, the dye-doped particles were collected by filtration with a membrane polycarbonate filter (ADVANTEC, pore size: 8 μm), washed, and desiccated. After that, they were dispersed in distilled water, and used for the experiments.

Dye concentrations in microparticles could not be measured directly, so they were estimated by the following experiment. PMMA (Mw: 5–10 $\times 10^5$) cast films were prepared from 5 wt.% PMMA/chloroform solution and were immersed in a Rh6G/methanol solution (10 ml, 1.0×10^{-2} M) or in a DODCI/methanol solution (10 ml, 1.0×10^{-3} M) for 48 h. The dye-impregnated PMMA films were washed, and desiccated. Then, the dye concentrations in PMMA films were determined from absorption spectra and thickness of films measured with spectrophotometer (SHIMADZU, UV-3100PC) and surface profiler (Sloan, DEK-TAK 3030), respectively. As a result, dye concentrations inside the particles were estimated to be 5.0×10^{-4} M for Rh6G and 5.0×10^{-5} M for DODCI, respectively. Rh6G- or DODCI- doped PMMA microparticles were also prepared in the same way and were used for the experiments.

2.2. Experimental setup

The experimental setup in this study is schematically illustrated in Fig. 1. The second harmonic (532 nm, fwhm ~ 30 ps) from a Q switched mode-lock Nd³⁺:YAG laser (EKSPLA, PL-2143-A) was used as a pumping beam. It was introduced into an optical microscope (Nikon, OPTIPHOT-2), and directed to individual microparticles through

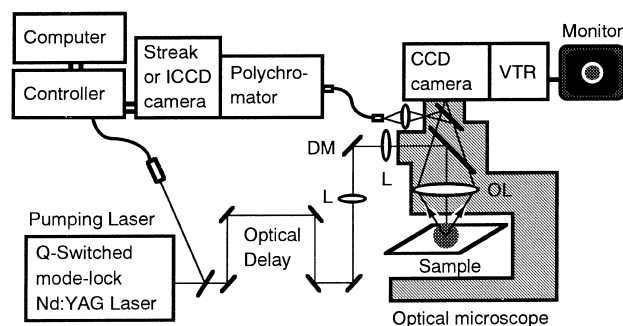


Fig. 1. A schematic diagram of an optical setup. DM: dichroic mirror, L: lens, OL: objective lens.

an objective lens (Nikon Fluor 40 \times , NA = 0.85). Emission from the microparticle was collected by the same objective lens, and analyzed by a polychromator (ORIEL, MULTI-SPEC 257) and detected by an ICCD camera (HAMAMATSU Photonics, C6394–01). Spectral resolution was 0.25 nm for a 300 lines mm^{-1} grating. For time-resolved measurements, a streak camera (HAMAMATSU Photonics, C4334–01) was used. A total time resolution of the detection system was ~ 50 ps. The behavior of the particle was monitored by a CCD camera which was attached to the microscope, and recorded by a video recorder.

3. Result and discussion

3.1. Emission spectra from Rh6G- or DODCI-doped microparticles

Emission from individual Rh6G-doped PMMA particles with various diameters was observed as shown in Fig. 2. Several distinct peaks were superimposed over fluorescent spectrum of Rh6G in each particle size (31, 48, and 56 μm). However, peaks were not observed above 610 nm. The intervals of these peaks ($\Delta\lambda$) were about 2.3, 1.5, and 1.3 nm for the particles with a diameter of 31, 48, and 56 μm , respectively (Table 1). According to the Mie scattering theory, the value of $\Delta\lambda$ is defined as follows [8–11]

$$\Delta\lambda = \frac{\lambda^2 \tan^{-1}(n^2 - 1)^{1/2}}{\pi n_2 d (n^2 - 1)^{1/2}}, \quad (1)$$

where λ is the peak wavelength, $n_1 = 1.49$ is the refractive index of the microparticle, $n_2 = 1.33$ is the refractive index

Table 1
Interval of the peaks for Rh6G-doped PMMA particles

| Diameter (μm) | Peak wavelength (nm) | Experimental value (nm) | Calculated value (nm) |
|----------------------------|----------------------|-------------------------|-----------------------|
| 31 | 580 | 2.3 | 2.3 |
| 48 | 580 | 1.5 | 1.6 |
| 56 | 580 | 1.3 | 1.3 |

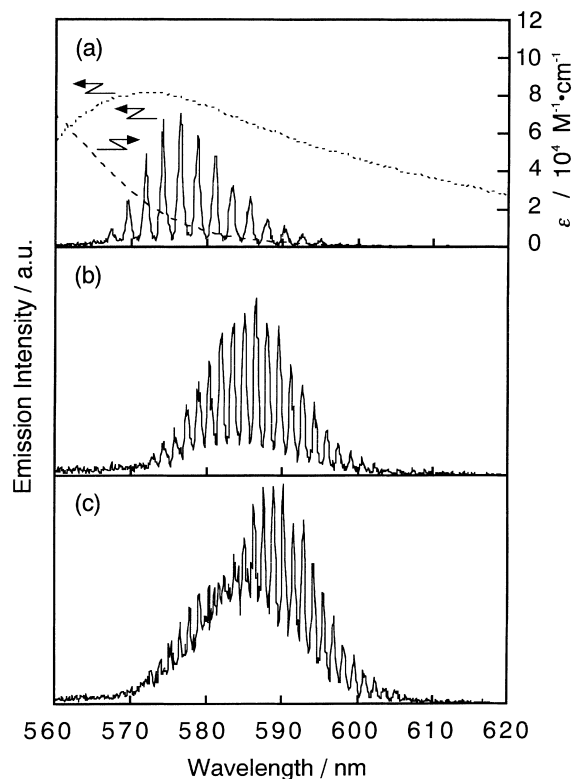


Fig. 2. Laser emission spectra (solid curve) of Rh6G-doped PMMA particles with fluorescence (dotted curve) and absorption (dashed curve) spectra of Rh6G-doped PMMA film. Diameter of particle: 31 μm (a), 48 μm (b), and 56 μm (c).

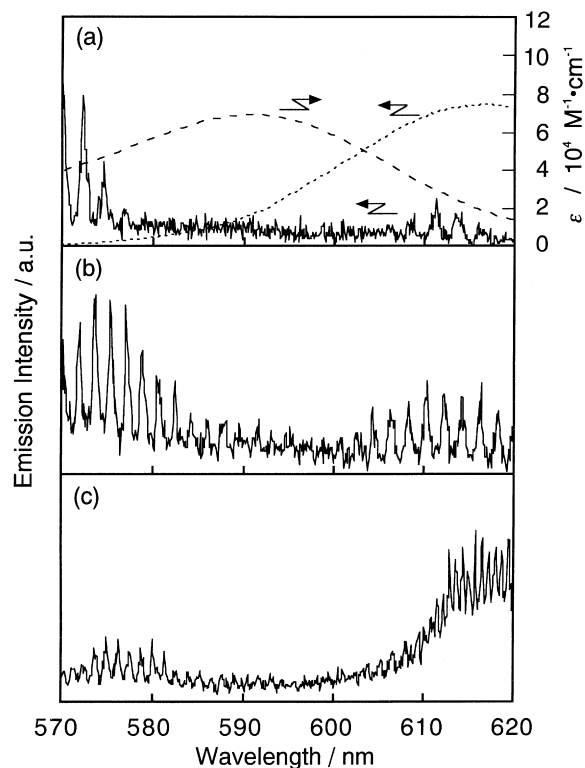


Fig. 3. Laser emission spectra (solid curve) of Rh6G–DODCI-doped PMMA particles with fluorescence (dotted curve) and absorption (dashed curve) spectra of DODCI-doped PMMA film. Diameter of particle: 30 μm (a), 40 μm (b), and 56 μm (c).

of the surrounding medium, $n = n_1/n_2$, and d is the diameter of the particle. The calculated values of $\Delta\lambda$ were about 2.3, 1.6, and 1.3 nm for the particles with a diameter of 31, 48, and 56 μm , respectively, and these values agreed well with the observed values within the resolution of the polychromator. Thus, it was concluded that these peaks were resonant peaks due to MDR in the micro-cavity. In the case of dye-doped microparticles lasing, not only (1) periodically spaced peaks, but also (2) nonlinear pump-power dependence of emission intensity and (3) shortening of emission decay time should be observed [5,8–10]. All these observations proof the peaks to be lasing peaks of micro-cavity. In addition, when the particle size becomes large, the wavelength region of lasing peaks are shifted to longer wavelength, since Q -value of the microparticle cavity becomes higher with the increasing diameter of particle, and, consequently, lasing threshold becomes lower. However, such increment in Q -value at the shorter wavelength range is suppressed due to reabsorption of dye. As a result, the maximum of lasing peaks shifts to the longer wavelength with increasing diameter of the particle.

On the other hand, lasing MDR peaks were not observed in DODCI-doped PMMA microparticles, and weak spontaneous emission band was observed at the same pumping power. This phenomenon is ascribed to weak absorption of DODCI at the pumping wavelength.

3.2. Particle cavity size dependence of the emission spectra in Rh6G–DODCI-doped PMMA microparticles

The individual particle of different diameters doped by both donor and acceptor dyes (Rh6G–DODCI-doped PMMA) was irradiated by the pumping laser beam ($0.64 \text{ J cm}^{-2} \text{ pulse}^{-1}$) and the emission spectra was measured as shown in Fig. 3. For each particle, the spectrum consisted of mainly two bands at 570–590 nm and 610–630 nm, and several sharp peaks were observed in the both spectral ranges. As shown later, these peaks were found to be lasing peaks. In the range of 610–630 nm, emission band was not observed for the Rh6G-doped PMMA particles (Fig. 2). Consequently, the 610–630 nm band was attributed to the emission from DODCI. The presence of the 610–630 nm band in Rh6G–DODCI-doped PMMA particles showed that an energy transfer from Rh6G to DODCI took place in these particles. On the other hand, in the range of 570–590 nm, emission band was not seen for the DODCI-doped PMMA particles, while the Rh6G-doped PMMA particles showed lasing peaks. From these results, the 570–590 nm band of the Rh6G–DODCI-doped PMMA particles was attributed to the emission from Rh6G. In the wavelength range of 590–610 nm, weak or no peaks were observed in the Rh6G–DODCI-doped PMMA particles, although Rh6G-doped PMMA particles showed several

Table 2
Interval of the peaks for Rh6G–DODCI-doped PMMA particles

| Diameter (μm) | Peak wavelength (nm) | Experimental value (nm) | Calculated value (nm) |
|----------------------------|----------------------|-------------------------|-----------------------|
| 33 | 580 | 2.1 | 2.3 |
| | 620 | 2.4 | 2.6 |
| 40 | 580 | 1.7 | 1.9 |
| | 620 | 2.0 | 2.1 |
| 56 | 580 | 1.2 | 1.3 |
| | 620 | 1.5 | 1.5 |

lasing peaks in this range. This is because the lasing of Rh6G was restrained by the absorption of DODCI at this wavelength range. Accordingly, the lasing peaks of the 610–630 nm band, which is not seen in DODCI-doped PMMA particles, were observed in Rh6G–DODCI-doped PMMA particles. These results indicate that an efficient energy transfer from excited Rh6G to DODCI in the microparticle cavity enables a lasing of DODCI.

The interval of the peaks around 580 nm was $\Delta\lambda = 2.4$, 2.0, and 1.5 nm, while those around 620 nm was $\Delta\lambda = 2.1$, 1.7, and 1.2 nm for the microparticles with diameter of 33, 40, and 56 μm , respectively (Table 2). The calculated values of $\Delta\lambda$ from the Eq. (1) around 580 nm were $\Delta\lambda_{\text{th}} = 2.6$, 2.1, and 1.5 nm and those around 620 nm were $\Delta\lambda_{\text{th}} = 2.3$, 1.9, and 1.3 nm. These values were found to be again in agreement with the experimental values within the resolution. Accordingly, we have concluded that these peaks were also resonant peaks due to MDR.

To confirm that the observed peaks were due to laser oscillation, the pumping power dependence of the resonance peak intensity was measured. The results for the Rh6G–DODCI-doped PMMA particle are shown in Fig. 4. As seen,

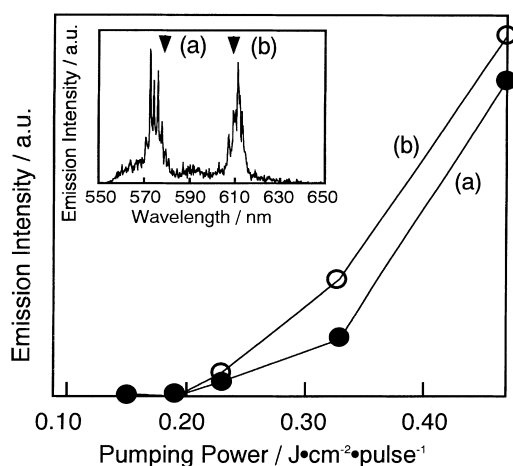


Fig. 4. Pumping power dependence of the emission peak intensity of Rh6G–DODCI-doped PMMA particle (diameter = 40 μm). The emission intensity was measured at 578.0 nm (a) and 609.4 nm (b). Inset: emission spectrum of the same particle.

the peak intensity at 578.0 nm, which was in the emission band of Rh6G, was not proportional to the pumping power, but increased rapidly when the power was larger than $0.19 \text{ J cm}^{-2} \text{ pulse}^{-1}$. This result clearly showed that origin of the emission peaks of Rh6G was not spontaneous emission, but induced emission due to the laser oscillation. In addition, the peak intensity was also increased in nonlinear way with the pumping power and intensity of Rh6G emission for the emission range of DODCI (609.4 nm), while the emission intensity increased linearly with the pumping power for the DODCI-doped PMMA particles. This result suggested that an efficient energy transfer between Rh6G and DODCI in microparticle cavity was inducing laser oscillation from DODCI.

As shown in Fig. 3, the intensity of the 610–630 nm emission band increased with the particle size, that is, the energy transfer efficiency was higher in the larger particles. This is caused by the following two reasons. First, the efficiency of the light confinement in the microparticle cavity was enhanced, that is, the Q -value was higher, for larger particles. Second, the wavelength region of Rh6G lasing peaks shifts to longer wavelength with the increase of the particles diameter as shown in Fig. 2 and overlapped with the absorption maximum of the DODCI. Consequently, it is concluded that the energy transfer efficiency in microparticle cavities can be controlled by the particle size.

This is a new technique to control the energy transfer. It is known that the energy transfer efficiency in homogeneous systems such as bulk solutions can be controlled by the dye concentration, temperature, dye orientation, and so forth. The present results show that the size is another parameter which affects the energy transfer efficiency in microparticle cavities. Hence, this technique is expected to be applied for new photonic devices such as a minute light source where emission wavelength range can be chosen.

3.3. Measurements of time-resolved emission spectra

Measurements of time-resolved emission spectra from donor and acceptor doped microparticles reveal the dynamics of energy transfer. However, picosecond time-resolved emission spectra from such particle cavities have not been reported so far. Thus, time-resolved emission spectra in the induced emission process were measured by using a streak camera. Fig. 5 shows time-resolved spectra, in which a spectral shift to longer wavelength with time is clearly seen. Fig. 6 shows time-profile of (a) pumping pulse, (b) emission of Rh6G, and (c) emission of DODCI. The peak of the emission of Rh6G comes ~ 20 ps after the peak of pumping pulse, and the peak of the emission of DODCI is ~ 50 ps after the peak of Rh6G emission, as shown in Fig. 6. The time constants of the decay curves, τ , were 10 and 63 ps for the lasing emission of Rh6G and DODCI, respectively. The precise analysis of the observed laser pulses by curve fittings with the rate equations was hampered by experimental errors ascribed to jitters and the

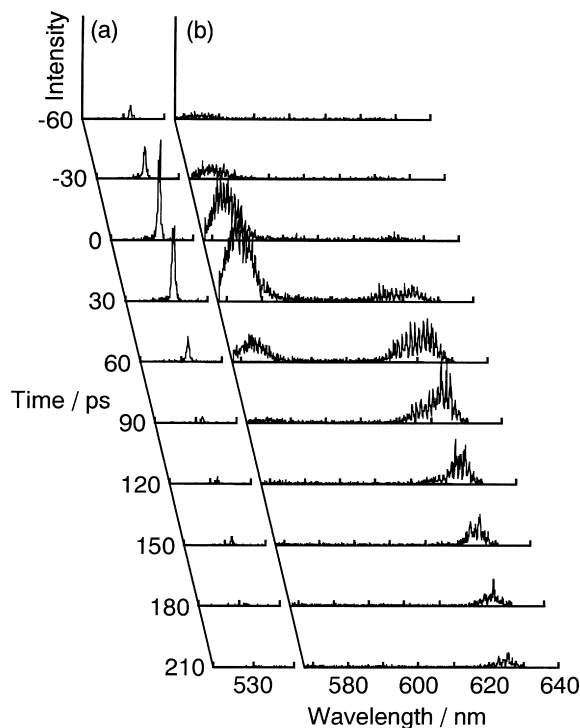


Fig. 5. Time-resolved spectra of pumping pulse (a) and emission of Rh6G–DODCI-doped PMMA particle (diameter = 55 μm) (b).

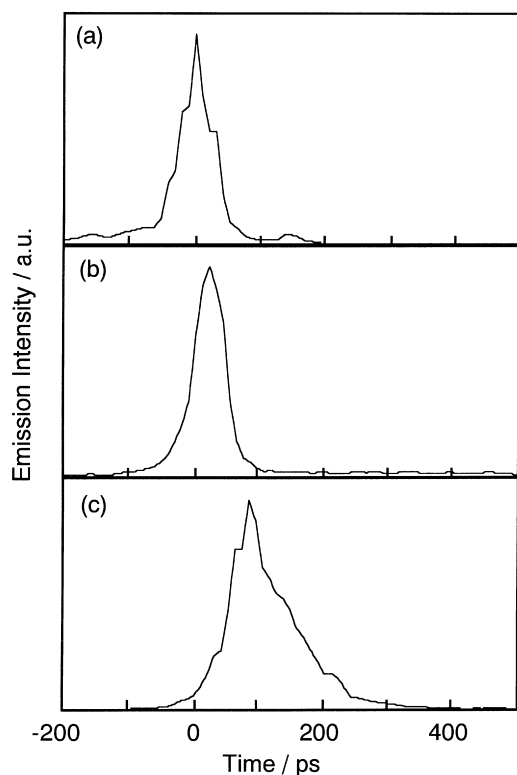


Fig. 6. Temporal profiles of pumping pulse at 532 nm (a), emission of Rh6G at 575–585 nm (b), and emission of DODCI at 621–625 nm (c). The same sample as in the case of data on Fig. 6. Each profile was normalized at its maximum.

fluctuation of measurement system. Therefore, experimental decay time constants were estimated as difference between pump and emission pulses of width at the height of $\exp(-1)$ [8].

In the particle cavities, the pulse light of induced emission is confined in the particle. Because the Q -value of such particle cavities is very high, light inside the particle decays mainly due to the reabsorption of the dyes present in the particle, rather than the loss at the total reflection. The time constant τ_a of the decay by the reabsorption is described as follows from the Lambert–Beer's law [8]

$$\tau_a = \frac{n_1}{\ln 10 \varepsilon(\lambda) a c}, \quad (2)$$

where $n_1 = 1.49$ is the refractive index of the particle, $\varepsilon(\lambda)$ is a molar extinction coefficient at the wavelength λ [$\varepsilon_{\text{Rh6G}}(580 \text{ nm}) = 9.4 \times 10^3 \text{ M}^{-1} \text{ cm}^{-1}$, $\varepsilon_{\text{Rh6G}}(620 \text{ nm}) = 0.3 \times 10^3 \text{ M}^{-1} \text{ cm}^{-1}$, $\varepsilon_{\text{DODCI}}(580 \text{ nm}) = 5.7 \times 10^4 \text{ M}^{-1} \text{ cm}^{-1}$, and $\varepsilon_{\text{DODCI}}(620 \text{ nm}) = 1.3 \times 10^4 \text{ M}^{-1} \text{ cm}^{-1}$], a is concentration of dyes ($a_{\text{Rh6G}} = 5.0 \times 10^{-4} \text{ M}$, $a_{\text{DODCI}} = 5.0 \times 10^{-5} \text{ M}$), c is the velocity of light in vacuum. From the equation, the time constant of decay is calculated as $\tau_a(580 \text{ nm}) = 3 \text{ ps}$ and $\tau_a(620 \text{ nm}) = 27 \text{ ps}$ considering an absorption by both donor and acceptor dyes. The values obtained experimentally were in agreement with the values calculated by Eq. (2) within the experimental error.

The peak of temporal profile of DODCI was late for $\sim 50 \text{ ps}$ in comparison with that of Rh6G, and the delay time was larger than the decay time constant of lasing of Rh6G ($\tau = 10 \text{ ps}$). This delay also indicates that DODCI was excited through the energy transfer from Rh6G. However, since the time profile under lasing condition is not proportional to the number of excited dyes, it cannot be judged whether the energy transfer occurs from reabsorption process or Förster mechanism.

4. Conclusions

In donor and acceptor doped PMMA microparticles, an enhanced excitation energy transfer from the donor dye of Rh6G to the acceptor dye of DODCI was observed under the lasing conditions. It was found that the energy transfer efficiency could be controlled by the particle size, whereas in the case of bulk materials it can be done controlling the dye concentration and temperature. Picosecond time-resolved spectral measurements revealed that laser oscillation of Rh6G was directly induced by the pump irradiation, and then that of DODCI occurred through an efficient energy transfer from Rh6G to DODCI.

Acknowledgements

The present work was partly supported by the Satellite Venture Business Laboratory of the University of Tokushima.

References

- [1] N. Ohta, N. Tamai, T. Kuroda, T. Yamazaki, T. Nishida, I. Yamazaki, *Chem. Phys.* 177 (1993) 591.
- [2] L.M. Folan, S. Arnold, S.D. Druger, *Chem. Phys. Lett.* 118 (1985) 322.
- [3] R.L. Armstrong, in: R.K. Chang, A.J. Campillo (Eds.), *Optical Processes in Microcavities*, World Scientific, Singapore, 1988, p. 257.
- [4] P.T. Leung, L. Young, *J. Chem. Phys.* 89 (1988) 2894.
- [5] K. Kamada, K. Sasaki, R. Fujisawa, H. Misawa, in: H. Masuhara (Ed.), *Microchemistry*, Elsevier, Amsterdam, 1994, p. 257.
- [6] H.M. Tzeng, K.F. Wall, M.B. Long, R.K. Chang, *Opt. Lett.* 9 (1984) 499.
- [7] M. Kuwata-Gonokami, K. Takeda, H. Yasuda, K. Ema, *Jpn. J. Appl. Phys.* 31 (1992) L99.
- [8] K. Kamada, K. Sasaki, H. Misawa, N. Kitamura, H. Masuhara, *Chem. Phys. Lett.* 210 (1993) 89.
- [9] H. Misawa, R. Fujisawa, K. Sasaki, N. Kitamura, H. Masuhara, *Jpn. J. Appl. Phys.* 32 (1993) L788.
- [10] K. Sasaki, H. Misawa, N. Kitamura, R. Fujisawa, H. Masuhara, *Jpn. J. Appl. Phys.* 32 (1993) L1144.
- [11] P.W. Barber, R.K. Chang, *Optical Effects Associated with Small Particles*, World Scientific, Singapore, 1988.
- [12] V.B. Braginsky, M.L. Gorodetsky, V.S. Ilchenko, *Phys. Lett. A* 137 (1989) 393.
- [13] M. Nagai, F. Hoshino, S. Yamamoto, R. Shimano, M. Kuwata-Gonokami, *Opt. Lett.* 22 (1997) 1630.
- [14] T. Takahashi, S. Matsuo, H. Misawa, T. Karatsu, A. Kitamura, K. Kamada, K. Ohta, *Thin Solid Films* 331 (1998) 298.
- [15] S. Arnold, L.M. Folan, *Opt. Lett.* 14 (1989) 387.